

## Supporting Information:

# Spin Crossover Molecular Ceramics by Cool-SPS: Consequences on Switching Features Beyond the sole Microstructural effect.

*Liza El-Khoury<sup>1</sup>, Nathalie Daro<sup>1</sup>, Guillaume Chastanet<sup>1</sup>, Dominique Denux<sup>1</sup>, Laetitia Etienne<sup>1</sup>, Vincent Mazel<sup>2</sup>, Michael Josse<sup>1</sup> and Mathieu Marchivie\*<sup>1</sup>.*

<sup>1</sup> Univ. Bordeaux, CNRS, Bordeaux INP, ICMCB, UMR 5026, F-33600 Pessac, France

<sup>2</sup> Univ. Bordeaux, CNRS, I2M Bordeaux, 146 rue Léo Saignat, F-33000 Bordeaux, France

### Table of content

<b>Table S1</b> Elemental analyses on different batches of powder 1.....	2
<b>Figure S1.</b> TEM image of [Fe(Htrz) <sub>2</sub> (trz)].BF <sub>4</sub> .....	2
<b>Figure S2.</b> $\chi_M T$ product versus T recorded on the “stabilized” cycle of (a) a powder and (b) a molecular ceramic of 1.....	2
<b>Figure S3.</b> Rietveld refinement results on the PXRD diagrams of [Fe(Htrz) <sub>2</sub> (trz)](BF <sub>4</sub> ) in the LS state at room temperature (a) before cycling and (b) after 20 cycles. ....	3
<b>Figure S4.</b> Sintering map of 1, presenting the conditions that did lead to molecular ceramics.....	3
<b>Figure S5.</b> (a) Diametral compression test and (b) Derivative of the elastic part response of the cold pressed pellets and SPS-processed ceramics. ....	4
<b>Figure S6.</b> Evolution of the hysteresis loop width ( $\Delta T$ ) for powder and molecular ceramics. ....	4
<b>Figure S7.</b> SPS monitoring.....	5
<b>Figure S8.</b> Fit of the magnetic measurements (VSM) for powder and molecular ceramic using the Slichter & Drikamer model. ....	5
<b>Figure S9.</b> Fit of the DSC peak in the warming mode for powder and molecular ceramic using the Sorai & Seki model. ....	5

**Table S1.** Elemental analyses on different batches of powder 1.

[Fe(Htrz) <sub>2</sub> (trz)](BF <sub>4</sub> )	% Fe <sup>(a)</sup>	% B <sup>(a)</sup>	% N <sup>(b)</sup>	% C <sup>(b)</sup>	%H <sup>(b)</sup>
Calculated values	16.0	3.1	36.1	20.6	2.3
Batch 1	14.7	3.5	34.7	20.1	2.3
Batch 2	14.5	3.4	34.5	20.1	2.3
Batch 3	14.7	3.4	34.3	20.0	2.3
Average exp. values	14.6	3.4	34.5	20.1	2.3

<sup>(a)</sup> ICP/OES analysis (Agilent ICP/OES 5800 DV). <sup>(b)</sup> Flash CHNS analysis (Thermo Fischer Scientific).

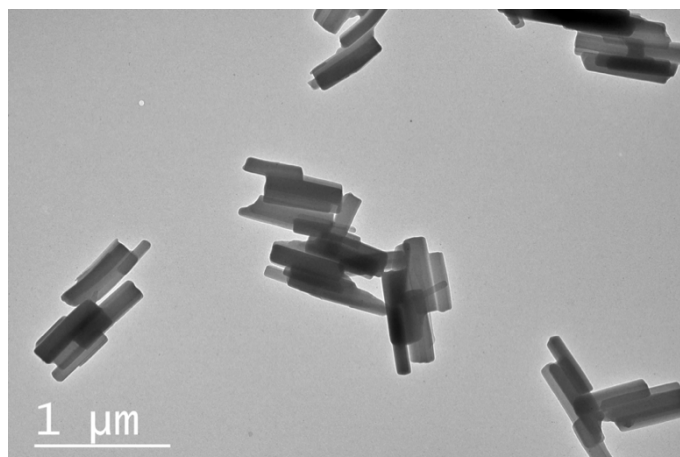


**Figure S1.** TEM image of [Fe(Htrz)<sub>2</sub>(trz)].BF<sub>4</sub> showing anisotropic particles with dimension ranging from 270 to 500 nm within the elongated direction and from 25 to 90 nm within the narrowest one.

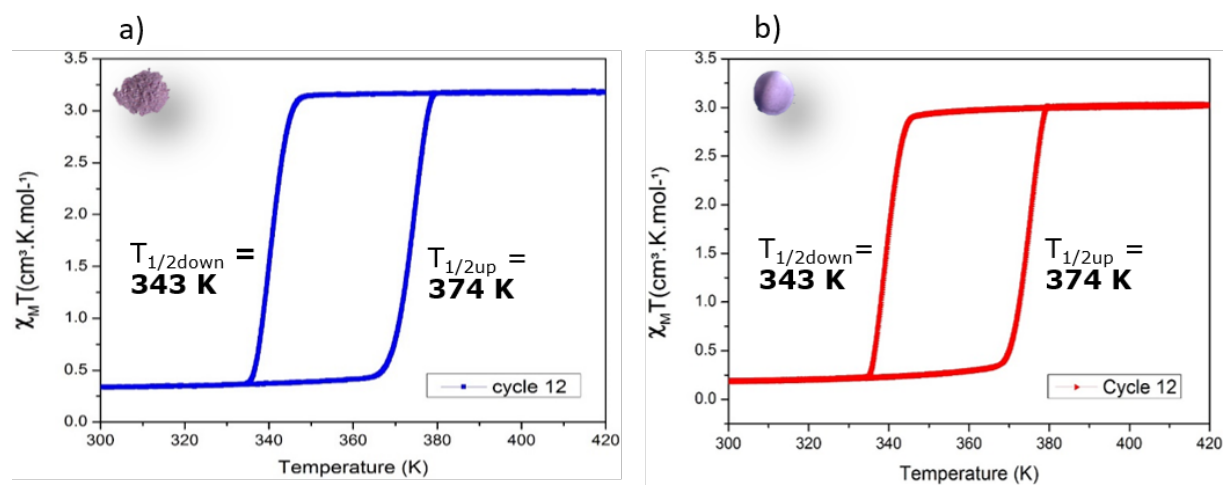


**Figure S2.**  $\chi_M T$  product versus T recorded on the “stabilized” cycle of (a) a powder and (b) a molecular ceramic of **1** showing the evolution of the magnetic properties and the transition temperatures.

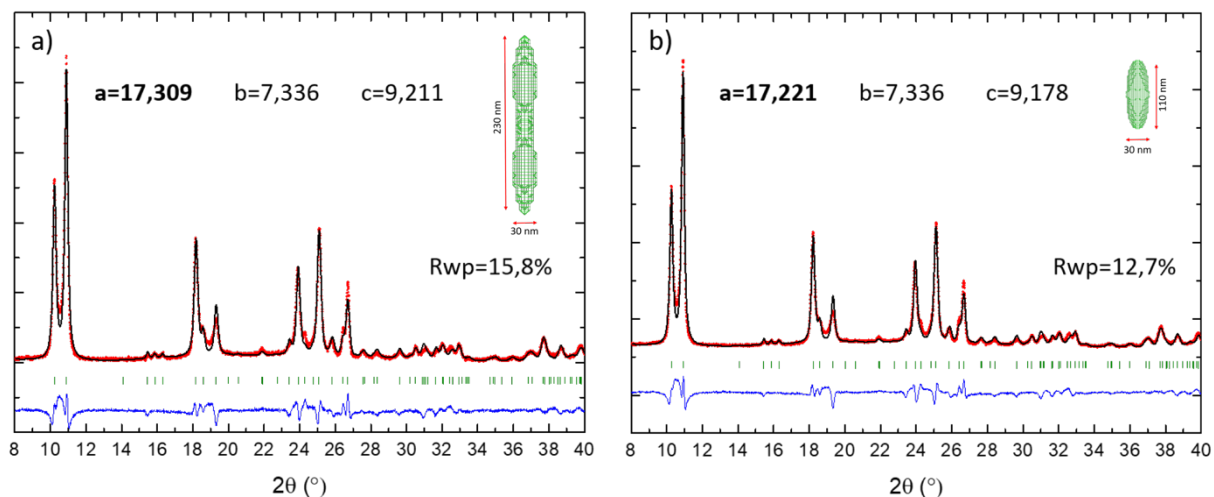


**Figure S3.** Rietveld refinement results on the PXRD diagrams of  $[\text{Fe}(\text{Htrz})_2(\text{trz})](\text{BF}_4)$  in the LS state at room temperature (a) before cycling and (b) after 20 cycles. Observed data (red circles), calculated diagram (black line) and difference curve (blue line). The anisotropic coherent domain sizes refined to 230 nm along the chain direction and 30 nm in the two other directions before cycling and to 110 and 30 nm respectively after cycling (insets).

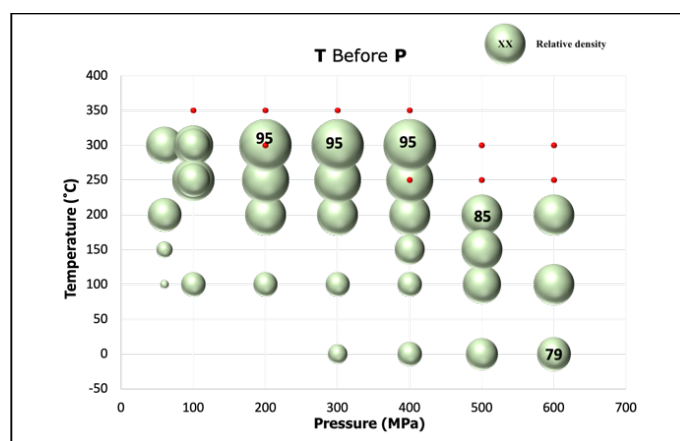


**Figure S4.** Sintering map of 1, presenting the conditions that did lead to molecular ceramics: applying temperature between 250 and 300°C before increasing pressure between 300 and 400 MPa. The size of the green symbols is proportional to the relative density of the obtained ceramics. Red dots indicate experiments which resulted in an altered sample.

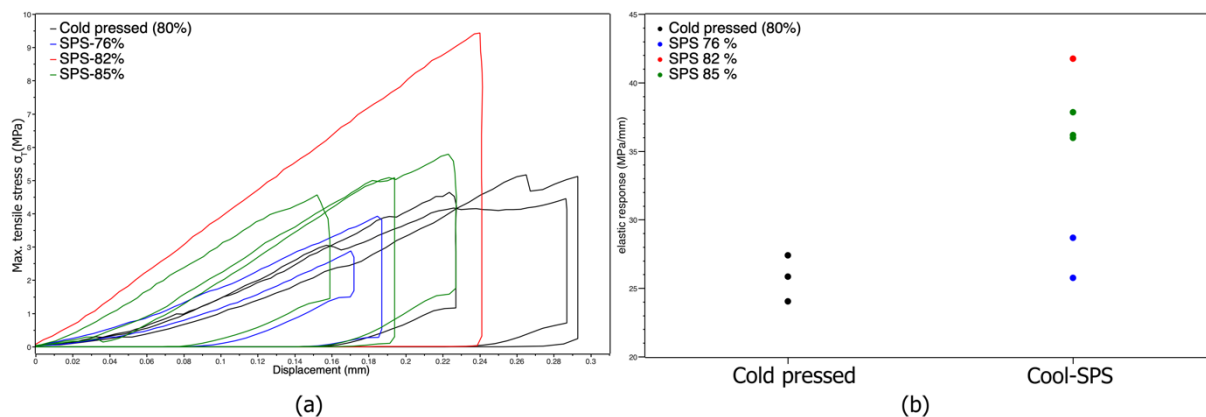


**Figure S5.** (a) Diametral compression test, showing that the molecular ceramic sintered by Cool-SPS (100°C/500MPa, 82% relative density) has the highest tear resistance and (b) Derivative of the elastic part response of the cold pressed pellets and SPS-processed ceramics. Percentage represent the measured relative density of the ceramics, cold pressed sample were measured at 80% of relative density.

As pellets could present inhomogeneous defects at the compressed surface the real breaking resistance tensile strength is difficult to estimate. The “elastic response”, that should be related to the elastic modulus has been thus preferred to compare cold pressed pellets and ceramics. The value of the “elastic response” for ceramics prepared by Cool-SPS systematically present higher values than cold pressed sample except when their relative density is lower.

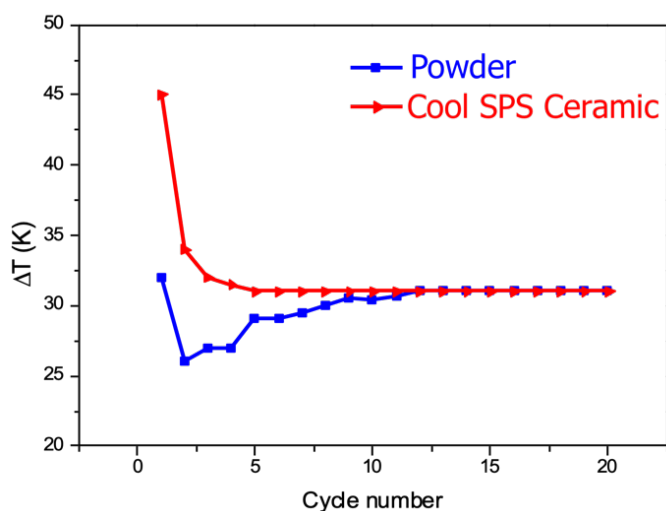


**Figure S6.** Evolution of the hysteresis loop width ( $\Delta T$ ) for powder (blue squares) and molecular ceramics (red triangles). Values obtained from DSC.

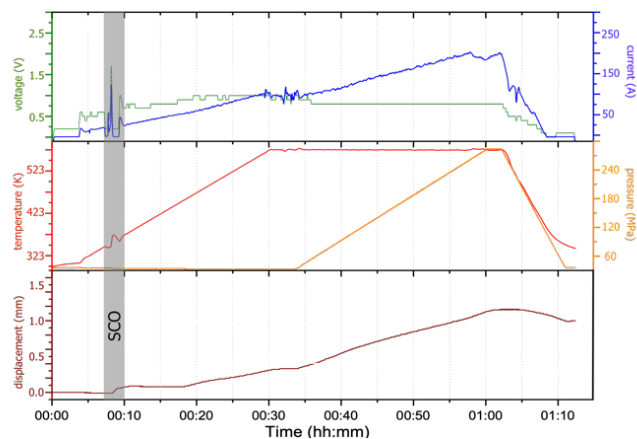


**Figure S7.** SPS monitoring showing the LS -> HS SCO signature around 380 K and 40 MPa in several experimental parameters (voltage in green, intensity in blue, temperature in red, displacement in brown).

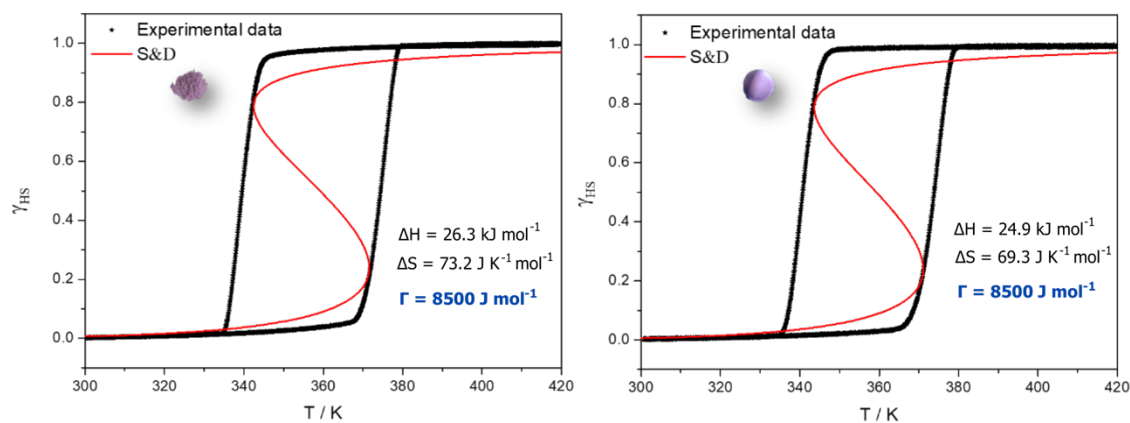


**Figure S8.** Fit of the magnetic measurements (VSM) for powder (left) and molecular ceramic (right) using the Slichter & Drikamer model.

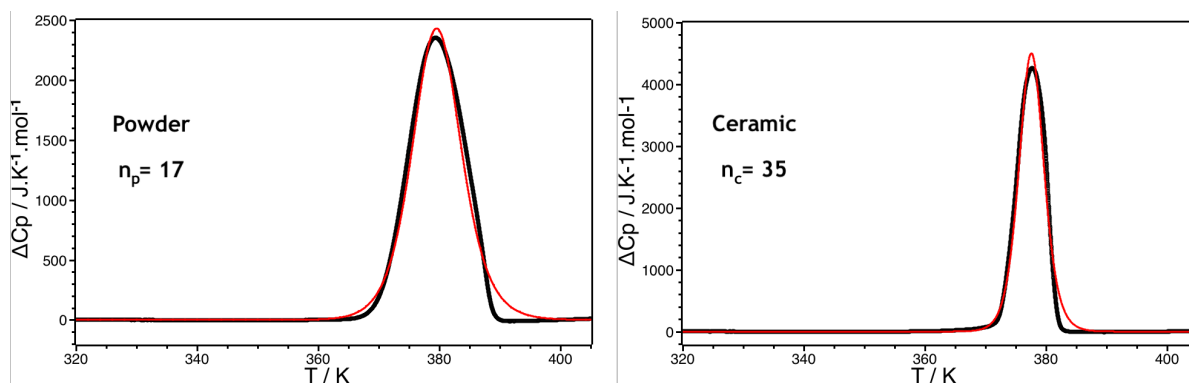


**Figure S9.** Fit of the DSC peak in the warming mode for powder (left) and molecular ceramic (right) using the Sorai & Seki

model. Using the equation : 
$$\Delta C_p = \frac{n \Delta H^2 e^{\frac{n \Delta G}{RT}}}{RT^2 (1 + e^{\frac{n \Delta G}{RT}})^2}$$